Dear Anonymous Referee #1,

Thank you for providing these detailed and insightful review comments. These comments will contribute to a much improved version of this research paper.

General Comments

Regarding the verification of wet snow and freezing of melt ponds with in-situ observations.

Direct *in-situ* verification was not possible since the Radarsat-2 acquisitions and aerial surveys were conducted over the Parry site, ~50km from the Field site, with field workers engaged in the survey and with landing on the melting ice surface not possible. However the wet snow and freezing pond explanations were closely ties to observations made nearly coincident in time and space. Further explanation is provided here.

Wet snow. Poor pond fraction estimation accuracy from Radarsat-2 scene R2 on 13 June (see Tab. 1) was attributed to a combination of wet snow and high wind speed (pond roughness) during acquisition. At best the wet snow condition was qualitatively verified at the Field site on the same day ~ 6h prior to the R2 acquisition over Parry site ~50km away. Unfortunately quantitative snow cover data including snow volumetric moisture content, collected by the snow pit method and detailed in Part 1 of this study, were discontinued on 13 June since the surface was a washed-out mixture of very shallow (<3cm) snow, slush, and newly forming pond cover types (see photo below). Measurement of the volumetric snow moisture content requires a minimum depth of 3cm to accommodate our measurement probe.

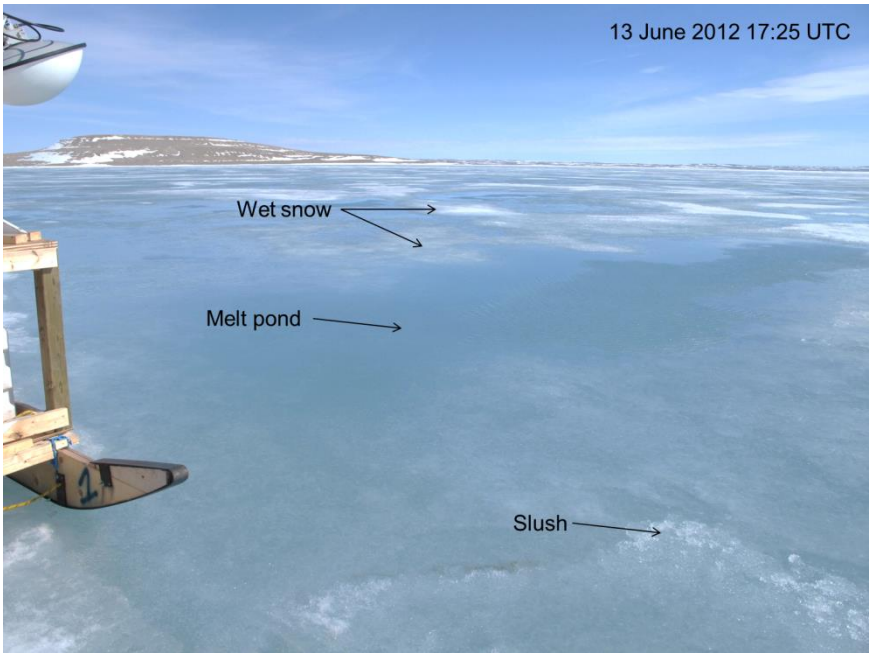

Figure 1. Remnant snow and slush patches observed with newly forming melt ponds at Field site on 13 June 2012.

There was a micro-meteorological station at Field site which recorded wind speed during the R2 acquisition on 13 June. However we chose to use data from the nearby Resolute

Environment Canada station for consistency, as it provided coincident data for all acquisitions in the study.

Freezing ponds. Poor pond fraction estimation accuracy from Radarsat-2 scene R4 on 24 June was attributed to freezing ponds. In-situ observations were made at Field site on the same day ~6h prior to the R4 acquisition and aerial survey, when the area was cloud covered and ponds were not observed frozen. The survey and R4 acquisition were conducted over Parry site after a clearing event, when ponds were visually observed to be frozen over (with the help of sun glint). The pond temperature and longwave flux data collected at Field (see Fig. 5) provide the best available verification.

Regarding an overview of sea ice conditions.

Added to section 3.1. where field study and location is already given.

Regarding the addition of more RS-2 or e.g. ENVISAT-ASAR APP images.

The addition of other SAR images is possible. However the study is highly dependent on the high resolution melt pond aerial imagery and derived melt pond information.

Regarding authors' view on relating PR to pond fraction or to albedo.

For a distributed target, the measured PR is closely related to pond fraction within the ideal radar-target configuration addressed in this study. Eicken et al. (2004) found that, for similar undeformed first-year ice near Barrow, the pond fraction is linearly related to the integrated surface albedo. As radar measured PR cannot account for variations in pond albedo due to controls such as pond depth, pond color (ice at pond base), and the presence of air bubbles at the pond base (Hanesiak et al., 2001), due to the negligible penetration depth of the radar into the water, it is more suitable to generally relate PR to pond fraction rather than albedo. As suggested, a discussion regarding this is added to the introduction section.

Regarding use of the IEM model.

Discussed below.

Regarding the Radarsat-2 image acquisition plan (new acquisitions and RS-2 archive).

The acquisition of scenes over the field site at 17 different times would have facilitated a more robust temporal evaluation of the technique. However the experimental design was driven by the need to take full advantage of aerial photography missions. By acquiring aerial photographs coincident to adjacent 25km by 25km scenes a much greater spatial distribution of pond fractions over the Parry Channel at each of the time intervals was made possible. Logistical constraints, namely flying conditions, would have made the acquisition of the aerial photos, essential for evaluating the technique, difficult. Similarly, though we agree that the inclusion of data from different years and locations (including the CIS archive) would increase the reliability of the results, validation requires accurate melt pond fraction

measurements as provided here by aerial photographs. A cross-comparison of melt pond fraction retrieval techniques using archived data, for example comparing the technique as applied to archived RS-2 images and the method of Rösel et al. (2012) as applied to co-located optical data from MODIS, would be very interesting and provide insights into the robustness of this technique. However such a study would still require high-resolution image data capable of discriminating melt ponds and providing 'verification' of melt pond fraction (e.g. aerial or tethered balloon photos).

Specific Comments

Introduction

P848/L20: Agreed. Text changed to highlight low spatial resolution as the primary problem in utilising these data for melt pond retrievals.

Regarding Scharien et al. 2007 study of PR vs. albedo relationship.

This work has been referenced in the introduction as suggested. As to the switch to PR vs. pond fraction, see the above comment regarding authors' view on relating PR to pond fraction or to albedo. The Scharien et al., 2007 was an empirical analysis, utilizing an albedo product, which provided the basis for the theoretically grounded and logical (linking PR to pond fraction instead of albedo) approach provided here.

2.2 Bragg scattering model

Cross-pol channels are zero.

This has been added to the text.

References for values of sea ice and melt pond permittivity.

References added.

IEM model approach.

Discussed below.

3.1. Data collection

P855/L20: Scene R1 is included in the study as it provides valuable baseline backscatter information (same radar-target configuration but prior to melting) from which to assess changes associated with ponding. The text has been modified to clarify that the R1 image was acquired prior to melting and that it is scenes R2 to R5 which are associated with AP imagery.

3.2 Data processing

Regarding radiometric resolution and absolute calibration accuracy.

Added to final version of manuscript.

P858/L3: Dimensions given in metres.

3.3 Pond fraction retrieval

Regarding noise, i.e. inaccuracy (±fraction).

Added to final version of manuscript, based on above radiometric resolution.

P859/L8: "Full resolution" meant collocated SAR PR and AP derived pond fraction data pairs collected from the 900 by 900m and 750 by 750m data blocks. This was to discriminate from data pairs later collected from the aggregated data (7.5 km grid cell). Since the use of "full resolution" is potentially misleading it has been removed and the text modified.

4.1 Seasonal evolution

P859/L23: Estimating variation due to incidence angle is difficult during ponding since the target parameters cannot be held constant; i.e. an equivalent pond fraction measured at two instances (incidence angles) are likely to include variations in backscatter caused by roughness and dielectric permittivity differences. For the final version of the manuscript an estimate using a suitable scattering model (likely IEM, see below) will be used.

P860/L9: In the case of smooth and thinly snow covered FYI, backscatter increases from wet snow relative to dry snow are attributed to a combination of surface and volume scattering mechanisms attributed to the melting process. These include scattering from enlarged melt-freeze snow clusters which are wetted by melt water (Barber et al., 1995) and increased scattering from rough features created by the re-crystallization of melt water draining to the snow-ice interface – i.e. ball-bearing ice (Drinkwater, 1989). However since variations in C-band single-polarisation backscatter during ponding is primarily a function of the melt pond fraction and surface wind speed (Comsio and Kwok, 1996; Yackel et al., 2007; Scharien et al., 2012), reference to "wet snow" has been removed.

P860, L14: This was explained in detail in Section 4.2. The lower PR observed for R4 was attributed to a surface cooling event detected nearby at the field site. The text has been updated to explain this better here.

4.2 Spatially distributed

Regarding Fig. 4.

The figure shows the coefficients of determination between PR/PR_x and pond fraction, i.e. information that would be provided by scatterplots (also discussed in the text). The decision

to display the transect data was based on the additional information on the polarization dependent nature of the target that can be taken from a relative comparison of the ratios.

P861/L18: The Bragg model was originally chosen for simplicity, i.e. by which to evaluate whether or not pond fraction could be retrieved from undeformed FYI without the need for wind speed or surface roughness information. However we agree that the larger validity range of the IEM model makes it a more appropriate model for the data analysis. We will re-do the analysis in the final manuscript and report the IEM model results instead.

Regarding PR_x and the RS-2 noise floor.

Assuming a worst case noise floor of -33.5 dB (noise floor of the FQP product is nominally -36.5 ±3 dB), the signal-to-noise ratio (SNR) of the HV channel is 5-7 dB during ponding and high enough that PR_x should not be contaminated. See below SNR histograms corresponding to coincident aerial survey and RS-2 statistics described on P858/L1-L10 (note: we used the aerial survey position overlay from AP4 on R1 since there was no aerial survey on that date; the orbit is similar to R5, which is paired with AP4). Mention is made in the revised manuscript here as suggested.

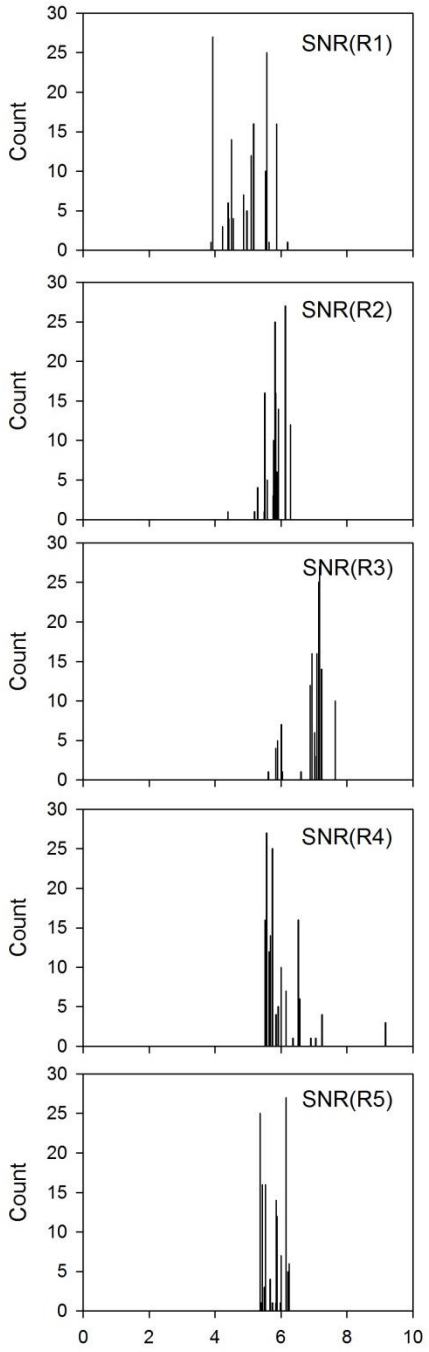

4.3 Pond fraction retrievals

P863/L9: Corrected reference to equation 9. “PR bands” refers to the VV/HH ratio bands created for each multiband product R1 to R5 as described on P856/L9-10. The text has been changed to clarify that Eq. 9 is being applied to each PR bands from R1 to R5.

P864,L15: This is a comparison of each pond fraction retrieval method (Bragg, Cscat – i.e. scatterometer, and CV). The text is updated for clarity.

P864,L16: Corrected.

5 Discussion

Regarding Sentinel-1 and RCM imaging modes.

> Clarification as to what will be available will be provided in the text; this has been suggested by both reviewers.

P866,L2: We will re-write this sentence for accuracy regarding the potential for noise floor issues in relation to conventional and future missions and include mention of utility of the ENVISAT APP scenes for this approach. Yes, RS-2 quad-pol data are scarce over sea ice and the data are at this stage experimental.

P866, L14: Howell et al. (2005) investigated the temporal evolution of the VV/HH ratio over landfast ice in the Canadian Arctic and found a similar strong PR response during melt relative to winter. The timing of PR in their work was largely compared to single-polarisation responses as in situ data on the ponding state were scarce.

Regarding application to QuickSCAT.

> A discussion will be added to the final manuscript on the potential for this approach to be applied to QuikSCAT data, including limitations regarding resolution, frequency (surface roughness effects) and incidence angle (inner/outer beams). Suggestions made by the reviewer regarding pack ice / ice deformation will also be included as is consistent with suggestions made by anonymous reviewer #2.

6 Conclusions

P867/L1: Corrected.

Technical Corrections

Fig. 2. Corrected.

Literature cited this document

Barber DG, Papakyriakou TN, LeDrew EF, Shokr ME. 1995. An examination of the relation between the spring period evolution of the scattering coefficient and radiative fluxes over landfast sea ice. *International Journal of Remote Sensing 16*(17): 3343–3363.

Comiso, J.C. and R. Kwok (1996), Surface and radiative characteristic of the summer Arctic sea ice cover from multisensor satellite observations, *J. Geophys. Res., 101*(C12), 28397-28416.

Drinkwater, M.R. (1989), LIMEX'87 ice surface characteristics: implications for C-band SAR backscatter signatures, *IEEE Trans. Geosci Remote Sen., 27*, 501-513.

Eicken, H., T. C. Grenfell, D. K. Perovich, J. A. Richter-Menge, and K. Frey (2004), Hydraulic controls on summer Arctic pack ice albedo, *J. Geophys. Res., 109*, C08007, doi:10.1029/2003JC001989.

Hanesiak, J.M., J. J. Yackel, and D. G. Barber (2001), Effect of melt ponds on first-year sea ice ablation-integration of RADARSAT-1 and thermodynamic modelling, *Can. J. Remote Sens., 27*(5), 433-442.

Howell, S.E.L., Yackel, J.J., De Abreu, R.A., Geldsetzer, T., and C. Breneman (2005), On the utility of SeaWinds/QuikSCAT for the estimation of the thermodynamic state of first-year sea ice, *IEEE Trans. Geosci. Remote Sens.,* 43(6), 1338-1350.

Scharien, R. K., J. J. Yackel, D. G. Barber, M. Asplin, M. Gupta, and D. Isleifson (2012), Geophysical controls on C band polarimetric backscatter from melt pond covered Arctic first-year sea ice: Assessment using high-resolution scatterometry, *J. Geophys. Res., 117*, C00G18, doi:10.1029/2011JC007353.

Yackel, J.J., D. G. Barber, T. N. Papakyriakou, and C. Breneman (2007), First-year sea ice spring melt transitions in the Canadian Arctic Archipelago from time-series synthetic aperture radar data, 1992-2002, *Hydrol. Processes, 21*, 253-265, DOI: 10.1002/hyp.6240.